Mechanical and electrical properties of acrylonitrile--butadiene rubber filled with treated nanographite

Doaa Essamey El-Nashar[1), *)], Nehad Naem Rozik[1)], Salwa Louis Abd El-Messieh[2)]

DOI: dx.doi.org/10.14314/polimery.2014.834

Abstract: Expanded, nano-scaled graphite treated with different mass ratios of poly(ethylene glycol) (PEG) (30, 50 and 70 wt %) were prepared. The prepared samples were investigated by Fourier Transform InfraRed spectroscopy (FT-IR), Transmission Electron Microscopy (TEM) and X-Ray Diffraction (XRD). Acrylonitrile-butadiene rubber (NBR) was loaded with graphite (G), expanded graphite (EG) and treated nanographite to prepare rubber composites and nanocomposites. The properties of the nanocomposites were investigated in terms of the cure characteristics, SEM, XRD, mechanical, electrical and thermal properties. The nanocomposites showed enhancements in cure characteristics and mechanical properties such as tensile strength, elongation at break, Young's modulus and hardness compared to the conventional composites filled with untreated graphite and unloaded NBR. The thermal stability of the NBR filled with treated nanographite was studied using thermogravimetric analysis (TGA), which showed an increase in thermal stability due to the presence of treated nanographite. The dielectric investigations reflected an increase in both the permittivity and dielectric loss with higher graphite contents and at a certain content, called the percolation threshold, an abrupt increase was noticed. The electrical conductivity (σ) was found to be in the order 10^{-10} Ω^{-1} cm^{-1}, which suggests these materials are suitable for antistatic applications.

Keywords: acrylonitrile-butadiene rubber, nanographite, nanocomposites, mechanical properties, electrical properties.

Mechaniczne i elektryczne właściwości kauczuku akrylonitrylo-butadienowego napełnionego różnymi rodzajami nanografitu

Streszczenie: Otrzymano nanokompozyty grafitu z różnym udziałem (30, 50 lub 70 % mas.) poli(glikolu etylenowego). Syntezowane próbki badano za pomocą spektroskopii w podczerwieni z transformacją Fouriera (FT-IR), transmisyjnej mikroskopii elektronowej (TEM) oraz dyfraktometrii rentgenowskiej (XRD). Następnie na bazie kauczuku akrylonitrylo-butadienowego (NBR) wytworzono kompozyty zawierające grafit (G), grafit ekspandowany (EG) lub grafit z udziałem poli(glikolu etylenowego). Oceniano właściwości termiczne, mechaniczne i elektryczne otrzymanych materiałów, wyznaczano charakterystykę ich sieciowania a także określano ich strukturę na podstawie zdjęć SEM. Stwierdzono, że nanokompozyty wykazywały lepszą charakterystykę sieciowania oraz właściwości mechaniczne, takie jak: wytrzymałość na rozciąganie, wydłużenie przy zerwaniu, moduł Younga i twardość, niż konwencjonalne kompozyty napełniane nieprzetwarzanym grafitem oraz nienapełniany NBR. Stabilność termiczną kauczuku NBR napełnionego układem grafit/poli(glikol etylenowy) badano z zastosowaniem analizy termograwimetrycznej (TGA); wykazano, że dodatek tak przetworzonego grafitu zwiększa stabilność termiczną kauczuku NBR. Stwierdzono zwiększenie przenikalności dielektrycznej i współczynnika strat dielektrycznych kompozytów wraz ze wzrostem zawartości grafitu, zaobserwowano też wzrost progu perkolacji. Wartości przewodności elektrycznej wytworzonych materiałów zawierają się w przedziale odpowiednim dla zastosowań antystatycznych.

Słowa kluczowe: kauczuk akrylonitrylo-butadienowy, nanografit, nanokompozyty, właściwości mechaniczne, właściwości elektryczne.

Nanocomposites are defined as composite materials where the reinforcement has one of the dimensions in the range of 1—100 nm. The most common nanoreinforcing agents used are layered silicates, nanoclays and carbon nanotubes. However, graphite platelets are also among the leading nanoscale fillers in research, development and commercial projects [1]. Many recent studies showed

[1)] National Research Centre, Polymers and Pigments Department, Al-Bohoos St., Dokki Post Number 12622, Dokki-Giza, Egypt.

[2)] National Research Centre, Microwave Physics and Dielectrics Department, Al-Bohoos St., Dokki Post Number 12622, Dokki-Giza, Egypt.

[*)] Author for correspondence; e-mail: doaaelnashar@yahoo.com, de.elnashar@nrc,sci.eg

that nano-scale, solid, lubricated fillers not only enhanced the mechanical properties but also significantly improved the wear resistance of polymers [2]. The nanomaterials are more effective reinforcements than their conventional counterparts because a smaller amount of nanomaterials causes a larger improvement of the matrix properties leading to lightweight composites and lower costs in many cases. In addition, the stress transfer from the matrix to the reinforcement is more efficient in the case of nanocomposites due to the high surface area, assuming good adhesion at the interface. Also, the crack propagation length at the interface becomes longer, improving the strength and toughness. New, nanoreinforcement, graphite-like nanoplatelets have recently attracted attention as a viable and inexpensive filler in composite materials [3] that can be used in many engineering applications thanks to the excellent in-plane mechanical, structural, thermal, and electrical properties of graphite. These excellent properties may be relevant at the nanoscale if graphite can be exfoliated into thin nanoplatelets and even down to a single graphene sheet [4]. Graphite nanoplatelets have often been made from expanded graphite, which was produced by heating graphite in a furnace at a temperature above 700 °C. This, in turn, was produced from graphite intercalation compounds *via* rapid evaporation of the intercalant at elevated temperatures then followed by a suitable treatment to produce treated nanoplatelets from the expanded material [5—7]. Exfoliated graphite has been used as a reinforcement material of polymers [3].

Poly(ethylene glycol) (PEG) [poly(ethylene oxide), PEOX] serving as a type of organic phase change material has been recommended as a thermal energy storage material due to its relatively high latent heat of 187 J/g, congruent melting behavior, better resistance to corrosion and suitable melting point [8—10]. Moreover, because PEGs are available with different molecular weights and melting temperatures, they can be used in many applications such as industrial heat utilization, electronic device management and protection, as well as in active and passive heating or cooling of buildings [11].

As is well known, in rubber reinforcement, the most important characteristic for the reinforcing filler is that it must be small, less than 0.0001 mm, so that the filler particles have a large surface area to interact with the rubber [12]. Besides the particle size, particle structure and surface chemistry are influential factors in determining the filler's reinforcing efficiency [13].

One of the largest areas of application for polymers and polymer composites are the electronic and electrical industries. Pure polymers are generally electrical insulators in their nature, so they are applied as electrically insulating materials. Polymers contain a very low concentration of free charge carriers, and thus they are non-conductive to electromagnetic radiation. For that reason they are not capable of being used as enclosures for electronic equipment as they cannot shield it from outside radiation or prevent the escape of radiation from the component. They also cannot provide protection against electrostatic discharge in handling sensitive electronic devices [14]. These drawbacks have led to the growth in the research for electrically conductive polymers. A critical concentration of filler, beyond which the polymer composite becomes conductive, is referred to as the percolation threshold. At this point a conductive network is formed through the matrix. This permits the movement of charge carriers in the fillers through the polymeric matrix, and so the composite achieves a certain degree of electrical conductivity. Numerous fillers can be compounded into the insulating matrix in order to achieve different conductivity ranges. Each filler can affect other properties besides conductivity, *i.e.* certain fillers are more appropriate than others for functioning in special applications. In electrical conductive polymers, the formation of the conductive network depends mainly on the filler concentration and geometry (and shape) [15—17].

In this study, samples treated with nano-scale graphite were prepared and characterized by different analytical techniques such as X-Ray Diffraction (XRD), Transmission Electron Microscopy (TEM) and Fourier Transform Infra-Red spectroscopy (FT-IR). The main goals of this work are to: (1) fabricate nanocomposites that contain modified-graphite in NBR (acrylonitrile-butadiene rubber) matrices; (2) determine the mechanical properties of the nanocomposites, *i.e.* tensile strength, elongation at break, Young's modulus and hardness and (3) evaluate the thermal and electrical properties according to the fillers.

EXPERIMENTAL PART

Materials

— Poly(ethylene glycol) (PEG) with molecular weight 1000 was purchased from Sigma-Aldrich USA.

— Graphite (G) (particle size: 20—30 μm) was purchased from the Al-Maghara coal mine in North Sinai (Jurassic), Egypt.

— Acrylonitrile — butadiene rubber (NBR) with bound acrylonitrile content of 32 %, specific gravity 1.17 ± 0.005 g/cm^3; was supplied by Bayer AG, Germany.

— *N*-cyclohexyl-2-benzothiazole sulphenamide (CBS), pale gray powder, with specific gravity of 1.27—1.31 g/cm^3 at room temperature (25 ± 1 °C), melting point 95—100 °C was used as an accelerator.

— Zinc oxide and stearic acid were used as activators with specific gravity at 15 °C of 5.55—5.61 g/cm^3 and 0.90—0.97 g/cm^3, respectively.

— Elemental sulfur, fine pale yellow powder, with specific gravity of 2.04—2.06 g/cm^3 at room temperature was used as a vulcanizing agent.

— Dioctyl phthalate (DOP) was used as a plasticizer with specific gravity 0.991 g/cm^3 and boiling point = 384 °C.

All the rubber ingredients were of commercial grades, purchased from Aldrich Co., Germany.

Graphite treatment

Graphite (G) was dried in a vacuum oven at 70 °C for 20 h and then the graphite was placed in a muffle at 900 °C for a few seconds to obtain expanded graphite (EG). The product was ground in a mortar into a fine powder and its average particle size was calculated by TEM. After that, poly (ethylene glycol) (PEG) was melted at 50 °C in a water bath. Later, the expanded graphite was added to the melted PEG. After mixing for 3 h, the composite was obtained and dried at room temperature. The composites were prepared at different mass ratios of PEG (30, 50 and 70 wt % of PEG) to graphite [11].

Preparation of NBR compounds loaded with untreated and treated graphite

The formulations of nitrile-butadiene rubber (NBR) compounds loaded with graphite (G), expanded graphite (EG) and graphite treated with PEG are given in Table 1. The compounds were prepared on two roll-mixing mills (outside diameter 470 mm, working distance 300 mm, speed of slow roll 24 rpm and friction ratio of (1:1.4) in accordance with ASTM D3182-07. The rubber compounds were vulcanized in an electrically heated hydraulic press at 152 ± 1 °C and a pressure of about 4 MPa for the optimum cure time (T_{c90}) as determined for each compound in Table 2.

Methods of testing

X-ray diffraction (XRD)

X-ray powder diffraction patterns were obtained at room temperature using a Philips diffractometer (type PW1390), employing Ni-filtered CuKα radiation (λ = 1.5404 Å). The diffraction angle, 2θ, was scanned at a rate of 2.5 °C/min.

Transmission electron microscopy (TEM)

The average particle size of pure graphite, as well as expanded graphite, was determined on a transmission electron microscope (TEM, JEOL JX 1230) equipped with a micro-analyzer electron probe.

Fourier transform infrared (FT-IR) spectroscopy

The FT-IR spectra of samples were obtained using a Jasco (Japan) FT-IR 430 series infrared spectrophotometer equipped with KBr discs.

Thermal gravimetric analysis (TGA)

TGA was conducted with a Shimadzu TGA-50H. A typical sample weight was about 8—10 mg and the analysis

T a b l e 1. Formulations of NBR compounds

Ingredient, phr*)	
NBR	100
Stearic acid	1.5
Zinc oxide	5
DOP**)	3
S (sulfur)	2
CBS***)	1.5
Graphite (G)	0, 2, 4, 6, 8 or 10
Expanded graphite (EG)	2, 4, 6, 8 or 10
Treated expanded graphite with 30 wt % PEG	2, 4, 6, 8 or 10
Treated expanded graphite with 50 wt % PEG	2, 4, 6, 8 or 10
Treated expanded graphite with 70 wt % PEG	2, 4, 6, 8 or 10

*) Part per hundred parts of rubber. **) Dioctyl phthalate.
***) *N*-cyclohexyl-2-benzothiazole sulphenamide.

T a b l e 2. Curing characteristics of the mixes at 152 ± 1 °C

Filler content, phr	M_L dNm	M_H dNm	T_{c90} min	t_{s2} min	*CRI* min^{-1}
Graphite (G)					
0	2	18	15	11	25
2	2	18	15	11	25
4	2	19	15	11	25
6	4	19	13	9	25
8	5	20	13	9	25
10	5	21	11	9	25
Expanded graphite (EG)					
2	3	20	13	10	33.33
4	5	23	11	9	50
6	6	24	10	8	50
8	8	28	9	8	100
10	7	26	11	9	50
Expanded graphite treated with 30 wt % PEG					
2	8	35	8	6	50
4	8	38	6	4	50
6	10	42	4	3	100
8	10	41	4	3	100
10	8	40	5	4	100
Expanded graphite treated with 50 wt % PEG					
2	7	30	8	7	100
4	9	31	8	7	100
6	10	35	6	5	100
8	9	34	7	5	50
10	7	33	7	5	50
Expanded graphite treated with 70 wt % PEG					
2	5	29	10	9	100
4	7	31	8	7	100
6	10	33	7	6	100
8	8	31	7	6	100
10	8	31	8	6	50

M_L — minimum torque, M_H — maximum torque, T_{c90} — optimum cure time, t_{s2} — scorch time, *CRI* — cure rate index.

was performed at a heating rate of 10 °C/min from 50 °C to 800 °C under a nitrogen atmosphere.

Rheometric and mechanical characteristics

The rheometric behavior of the rubber compounds was determined using an oscillating disc, Monsanto rheometer model 100, according to ASTM D2084. The vulcanized sheets prepared for mechanical tests were cut into five individual dumb-bell shaped specimens by a steel die of constant width (4 mm). The thickness of the test specimen was determined by a gauge calibrated in hundredths of a millimeter. A working part of scale 15 mm was chosen for each test specimen. The mechanical properties (*e.g.* tensile strength, elongation at break and Young's modulus) of the rubber compounds were determined according to standard methods using an electronic Zwick tensile testing machine, model 1425, in accordance with ASTM D412. Hardness was measured using a Shore A durometer according to ASTM D2240.

Dielectric measurements

Dielectric measurements were carried out in the frequency range 100 Hz up to 100 kHz by using a LCR meter, type AG-411 B (Ando electric Ltd. Japan). The capacitance *C*, the loss tangent tanδ and the resistance *R* were obtained. The samples were molded in the form of discs 5 cm diameter and 3 mm thickness. A guard ring capacitor (type NFM/5T Wiss Tech. Werkstatten GmbH, Germany) was used as a measuring cell. The cell was calibrated with standard materials [18] and the experimental errors in ε' and ε'' were found to be ± 3 and ± 5 %, respectively.

RESULTS AND DISCUSSION

Characterization of the graphite treatment

X-ray diffraction

Figure 1 illustrates the XRD patterns of graphite (G), expanded graphite (EG) and modified nanographite with PEG (30, 50 and 70 wt %), respectively. One can see from (Fig. 1) that graphite G shows a characteristic diffraction peak at 2θ = (24.55° and 44.6°) [2, 19], which is assigned to the interlayer platelet spacing. However, a displacement of the peak to lower angles 22.62° and 42.33° occurs for EG, 21.3° and 37.52°; 21.55° and 40.22°; and 21.91° and 39.3° for nanographite modified with 30, 50 and 70 wt % of PEG, respectively. These results correspond to an interlayer d-spacing of 2.42 nm and 3.45 nm for G, 8.52 nm and 5.9 nm for EG while the modified nanographite with 30, 50 and 70 wt % of PEG are observed at 9.08 nm and 6.65 nm, 8.93 nm and 6.19 nm, and 9.5 nm and 6.13 nm, respectively, as deduced by the Bragg's equation. The results indicate the successful formation of the intercalated graphite with treated G.

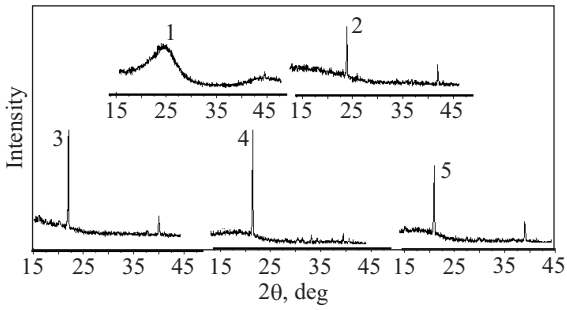

Fig. 1. XRD patterns of: 1 — untreated graphite, 2 — expanded graphite, 3 — treated expanded graphite with 30 wt % PEG, 4 — 50 wt % PEG, 5 — 70 wt % PEG

Thus, the X-ray diffraction data of the products indicate that PEG allows the EG molecules to migrate between the layers [19].

Transmission electron microscopy

Transmission electron micrographs for the graphite, expanded graphite and treated nanographite (30, 50 and 70 wt % of PEG) are presented in Fig. 2a—e. It is clear from these figures that the particle diameters are measured as 36 μm, 28 nm, 13.7 nm, 19 nm and 21 nm for G, EG and treated nanographite (30, 50 and 70 wt % of PEG), respectively. The transmission electron micrographs confirm the XRD results [20, 21].

FT-IR spectroscopy

FT-IR measurements were carried out as shown in (Fig. 3-1). It is clear that there is a peak at the wave number 1107 cm^{-1} caused by the stretching vibration of C-O. Additionally, a peak caused by the stretching vibration hydroxyl group O-H is also found at 3445 cm^{-1}. Peaks at 2921 cm^{-1} and 946 cm^{-1} represent the stretching vibration of -CH_2 and crystal peak of PEG. From (Fig. 3-2), the FT-IR absorption spectrum of PEG/EG composite was compared to that of pure PEG. It is found that the main peak is slightly shifted. The peak of functional group of C-O appeared at 1107 cm^{-1} and 1114 cm^{-1}. The group of -CH_2 is found at 2889 cm^{-1} and 951 cm^{-1}. The peak of functional group of O-H appears at 3445 cm^{-1} and 3457 cm^{-1}. The frequency of the composite main group shifts mentioned means that there is an interaction between PEG and EG.

Characterization of the nanocomposites

X-ray diffraction

The XRD pattern for nanocomposites of NBR with 6 phr EG and 6 phr modified nanographite with 30 wt % of PEG does not show any diffraction peak, Fig. 4. This suggests that the rubber entered into the graphite interlayer spacing and separated the graphite nanolayers to form an exfoliated structure in such a way that the

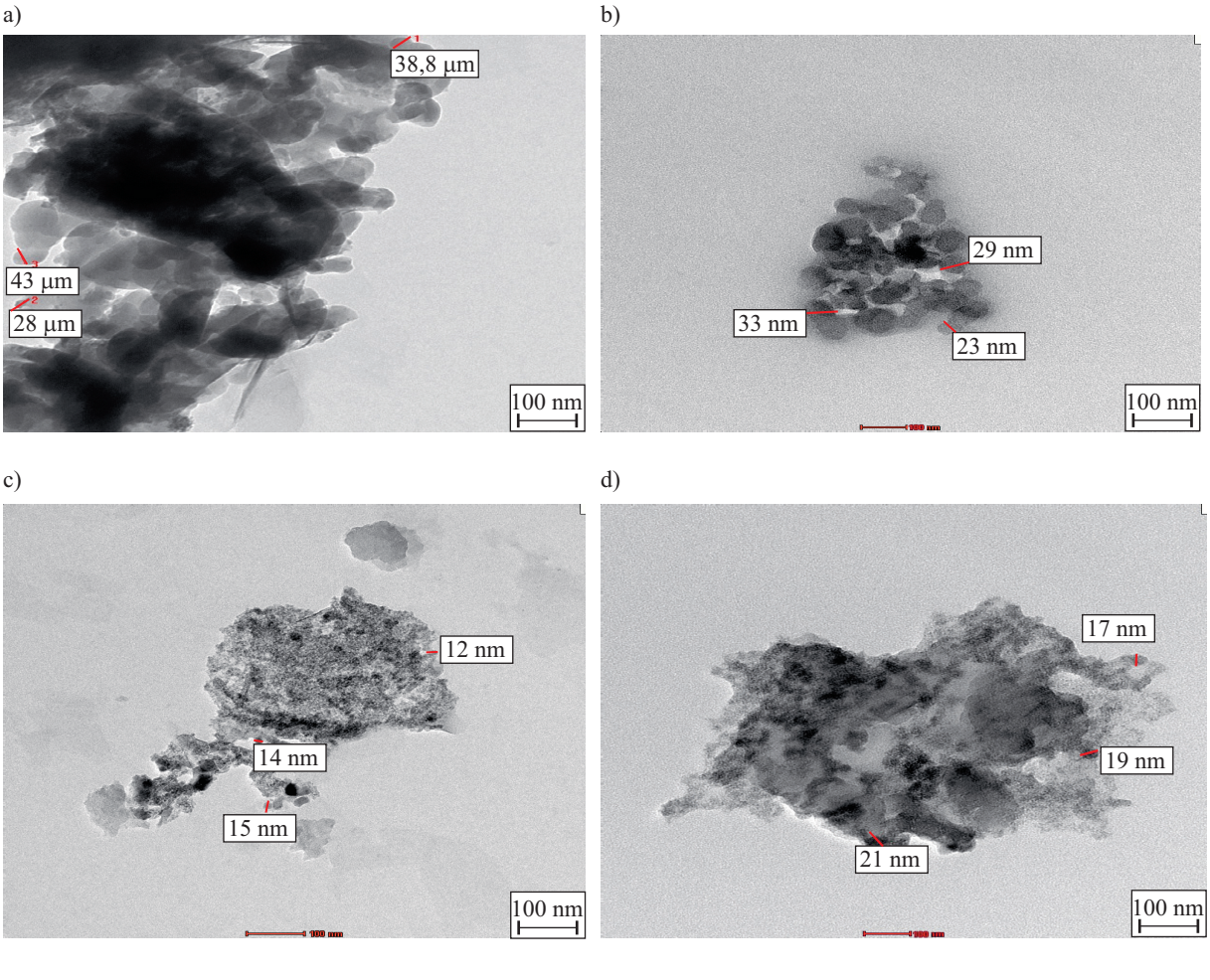

Fig. 2. TEM images with magnification 1000× of a) graphit, b) expanded graphite and treated expanded graphite with: c) 30 wt % PEG, d) 50 wt % PEG, e) 70 wt % PEG

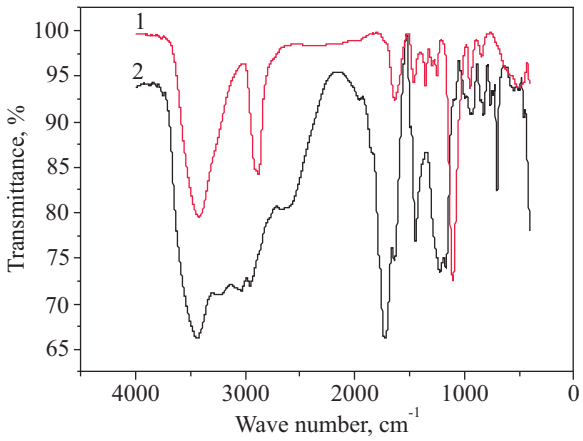

Fig. 3. FT-IR spectra of: 1 — poly(ethylene glycol), 2 — graphite/poly(ethylene glycol) (50/50)

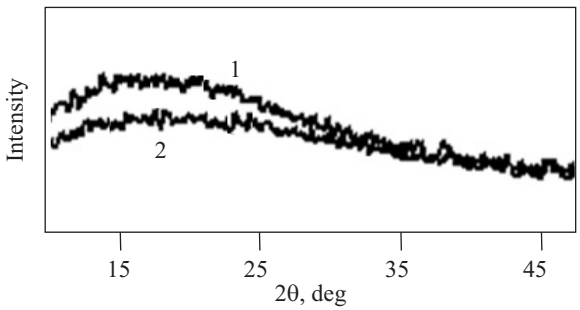

Fig. 4. XRD patterns of: 1 — NBR/6 phr EG, 2 — NBR/6 phr expanded graphite treated with 30 wt % PEG

Bragg's diffraction peak cannot be obtained, or the graphite nanolayers could have randomly dispersed in the polymer matrix, which is called an exfoliated structure. Hence, the XRD pattern confirms the formation of exfo-

liated nanocomposites [19, 22] at graphite content lower than 6 phr. The nanocomposites produced will be used as a reinforcing agent in rubber compounds.

Cure characteristics

The cure characteristics of the polymer are important where the product is to be molded. The processability of composites can be determined by evaluating the cure characteristics such as minimum torque M_L, maximum torque M_H, scorch time t_{s2}, and optimum cure time T_{c90}. Evaluation of the cure time for curing compounds and the variations in cure time for different loadings were studied for nitrile rubber composites containing different concentrations of G with micro-scale and nano-scale EG and treated nanographite (30, 50 and 70 wt % PEG).

Minimum torque (*i.e.* the torque at the initial stage of vulcanization) is related to the viscosity of the compounds. Minimum torque of the composites loaded with different concentrations of micro-scale graphite, nano--scale of EG and treated nanographite are shown in Table 2. The minimum torque increased with loadings of either micro-scale G at 10 phr, nano-scale EG and treated graphite up to 8 phr and 6 phr, respectively. Then, the minimum torque decreased with further loading but in the case of composites containing micro-scale graphite it shows lower values than those loaded with nano-scale of EG graphite and treated graphite. As the torque is directly proportional to stiffness, the results indicated that increasing the content of nano-scale EG and treated nanographite in the rubber matrix increases the stiffness of the vulcanizate [3, 13, 23].

The maximum torque gives an idea about the shear modulus of the fully vulcanized rubber at the vulcanization temperature, which increases with filler loading [23]. It can be clearly detected that the maximum torque increases with increased graphite loading in the composite but in the case of composites loaded with nano-scale EG and treated graphite the maximum torque increased up to 8 phr and 6 phr, respectively, before decreasing. This increase was an indirect hint for improved interfacial adhesion between NBR and nanographite. Upon a further increase in nanographite loading (*i.e.* 10 phr) and agglomeration of the filler in the NBR matrix, these observations confirmed that the addition of treated nano-scale graphite in nitrile rubber affects the processability of the composite and hence the treated graphite can act as a reinforcement agent for the matrix.

The variations of scorch and cure times with the loading of different graphites in NBR are also shown in Table 2. The addition of micro-scale graphite reduces both the scorch and cure times but for composites loaded with nano-scale graphite the scorch time t_{s2} and optimum cure time T_{c90} decreased with the addition of nano-scale graphite up to 8 phr and 6 phr for nano-scale EG and treated nanographite, respectively, before increasing. This decrease is due to the stronger interaction between nanographite and NBR matrix produced from the high surface area possessed by these fine size particles, which lead to a softening effect, and the main reason for this decrease is due to the homogenous distribution of this nanographite in the NBR matrix. Consequently, this led to advanced productive efficiency and a saving in processing energy. The increasing of t_{s2} and T_{c90} after 8 phr and 6 phr for nano-scale graphite may be due to the agglomeration of nanographite particles, or simply the result of physical contact between adjacent agglomerates. The agglomerate becomes a domain that act as a foreign body in the composites. The presence of a high amount of agglomerates in higher nanographite loadings act as obstacles to chain movements and thus lower rheometric characteristics will be obtained [13, 23]. An upward trend was observed with the cure rate index (*CRI*) (rate of curing reaction) as represented in Table 2. This increase is more pronounced in the case of modification with PEG and may be due to the strong improvement of the interfacial rubber-filler interaction that leads to an enhancement in rheometric properties.

Mechanical properties

The mechanical properties of NBR vulcanizates loaded with different concentrations of fillers (G with micro--scale, EG and treated graphite with nano-scale) are displayed in Fig. 5a—d. The mechanical properties include tensile strength (TS_b), elongation at break (E_b), Young's modulus (Y) and hardness (H) of composites.

The low reinforcing effect of unmodified graphite is evident, which confirms that a conventional composite at the micro-scale has been formed. However, the rubber samples loaded with both EG and modified nanographite exhibit higher tensile strength, elongation at break, Young's modulus and hardness than those samples loaded with unmodified graphite, Fig. 5a-d. As expected, these improvements in the mechanical properties, at low concentrations of both EG and modified nanographite, are due to the nano scale structure of the modified graphite. The nanocomposite samples loaded with 4—6 phr of EG and modified nanographite showed the highest mechanical strength properties. The increase of elongation indicates the softening effect of the modified graphite in rubber compounds. The enhancement in the mechanical properties suggests a strong interaction between matrix and modified graphite.

EG was treated with PEG to give a better distribution in the NBR matrix. It is well known that the distribution of filler in a rubber matrix is one of the most important factors affecting the physical properties of the final products [24].

PEG was used as a dispersing agent for improving the distribution of EG in the NBR matrix. In the nanocomposites, a higher PEG dispersion causes exfoliation of graphite, leading to thinner graphite sheets, better graphite-rubber interface adhesion and better rubber rein-

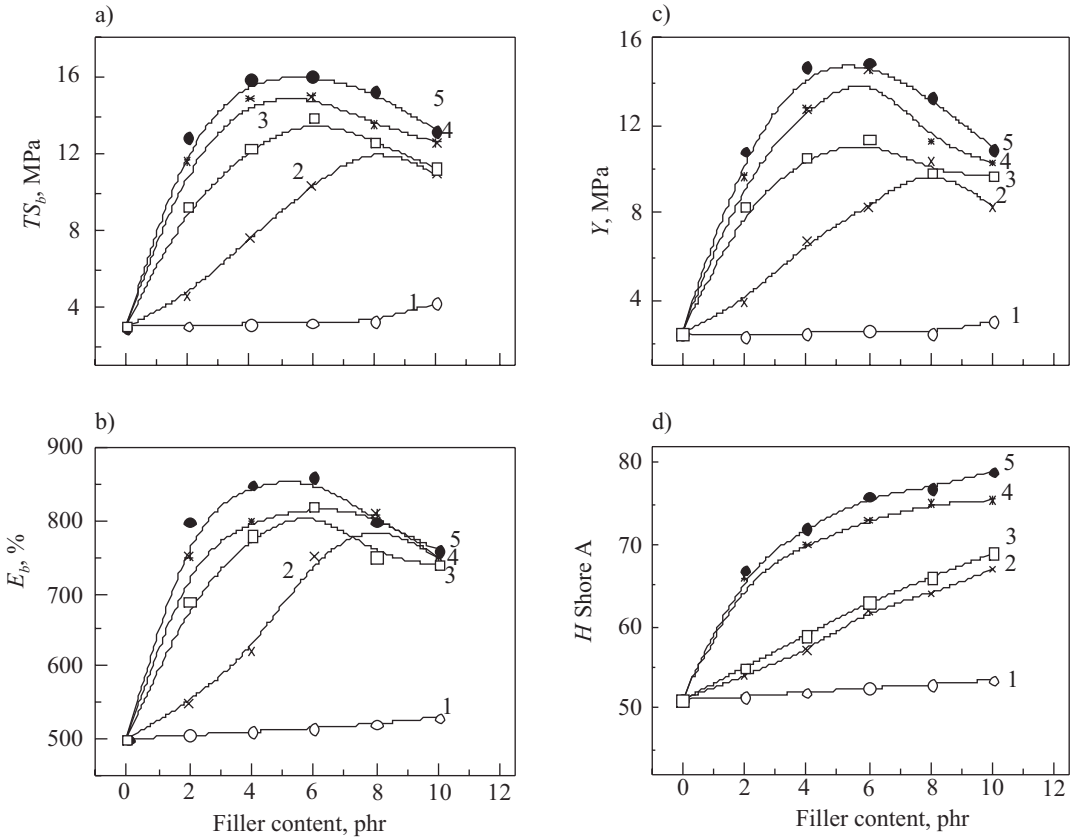

Fig. 5. Effect of fillers loading on mechanical properties of NBR vulcanizates: a) tensile strength (TS_b), b) elongation at break (E_b), c) Young's modulus (Y), d) hardness (H): 1 — G, 2 — EG, 3 — 70 wt % PEG, 4 — 50 wt % PEG, 5 — 30 wt %

forcement, as shown in Fig. 5c, d, as well as indicating that the nanographite layers were exfoliated in the rubber matrix. These findings were confirmed by XRD analysis.

Even a small increase in the amount of nanographite up to 6 phr for treated nanographite and 8 phr for EG will lead to significant increases in the strength, elongation at break, Young's modulus and hardness of the composites loaded with untreated G and treated nanographite can be ranked as follows:

30 wt % PEG > 50 wt % PEG > 70 wt % PEG > EG > G

A larger specific surface and facilitated physical interactions between graphite and polymer due to the functional groups explains this ranking [3].

Dispersion of graphite G leads to thick sheets, poor interfacial adhesion, low tensile strength, elongation at break, Young's modulus and hardness [2, 22].

Lower tensile strengths measured for samples above 6 phr and 8 phr nanographite loading can be attributed to the inevitable aggregation of the graphite layers at high nanofiller content. This may be because ductility decreases when stiffness is increased by reinforcement [23, 24].

Thermal properties

Thermal degradation studies involve the measurement of the changes in weight of the polymeric material as a result of heating in the presence of an inert atmosphere or in the presence of air/oxygen [25].

The thermogravimetric plots of unfilled NBR, and NBR loaded with 6 phr of treated nanographite with 30 and 50 wt % of PEG are given in Fig. 6. From this figure it was observed that the thermal degradation of NBR occurs *via* two-stage mechanisms due to the presence of acrylonitrile and butadiene monomer units. The first

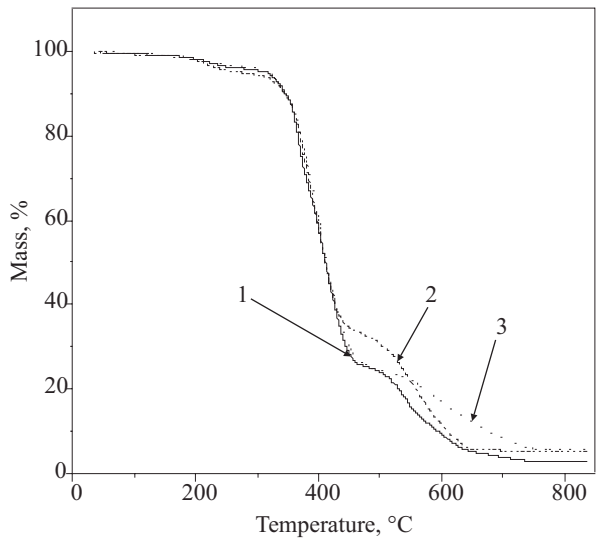

Fig. 6. TGA curves of: 1 — NBR, 2 — NBR/6 phr expanded graphite treated with 30 wt % PEG, 3 — NBR/6 phr expanded graphite treated with 50 wt % PEG

stage of degradation from 310 to 460 °C is mainly due to the degradation of butadiene, whereas the second stage of degradation that occurs in the region 460—553 °C is mainly attributed to the degradation of acrylonitrile monomer units.

Mass losses of 84 and 12 % are observed during the first and second stages of degradation, respectively.

It can also be seen that the thermal degradation curves of NBR samples loaded with 6 phr of treated nanographite with 30 and 50 wt % of PEG shift towards higher temperature by delaying the maximum degradation temperature, *i.e.* more stable, and more residues are retained [21, 25].

Samples loaded with 6 phr of treated nanographite with 30 wt % of PEG exhibit the highest thermal stability and the lowest rate of mass loss (residue is 6 %) which resulted in a high residue at high temperature when compared with samples loaded with 6 phr of treated nanographite and 50 wt % of PEG (residue is 5.34 %) and NBR (residue is 3 %).

Dielectrical properties

The permittivity ε′ and dielectric loss ε″ were measured in the frequency range from 100 Hz up to 100 kHz and at 30 °C for NBR loaded with graphite and various concentrations ranging from 0 up to 10 phr before and after treating with PEG.

Figure 7 displays the plots of ε′ and ε″ versus frequency for the NBR loaded with various contents of G as received and EG ranging from 0 to 10 phr at 30 °C. It can be seen that the permittivity ε′ of the composites decrease as a function of increased applied frequency, indicating anomalous dispersions. Also, the values of ε″ are broad, indicating that more than one relaxation mechanism as expected. It is well known that the main contributions to the ε″ values of the composites are two polarizing processes. The first is an interfacial polarization, which was induced through a local accumulation of free charges captured by defects or interfaces in the composites. This is related to the Maxwell Wagner effect due to differences in the permittivity and conductivity of NBR and graphite. The second process reflects the polarization of various scaled dipoles [26].

The values of ε″ in the low frequency range are due to the contribution of both interfacial polarization and conductivity, while the increase in ε″ at higher content of G is mainly due to the increase in electrical conductivity [27]. The values of ε′ and ε″ given in Fig. 7 at the different frequencies indicate that an abrupt increase is noted when

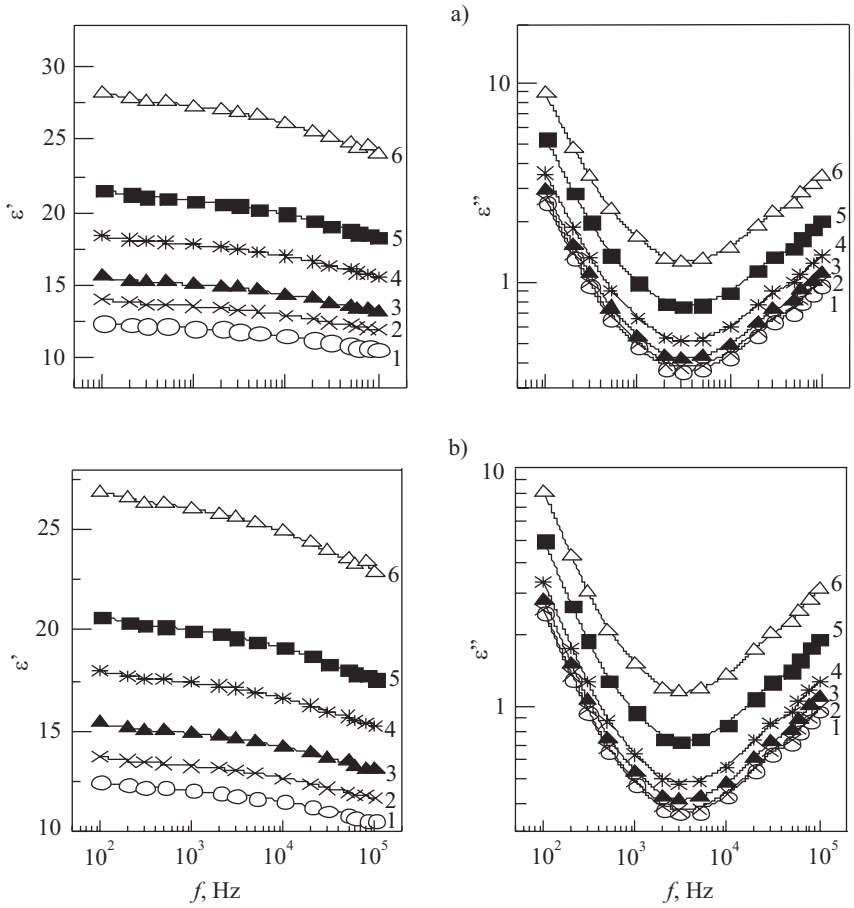

Fig. 7. The permittivity (ε′) and dielectric loss (ε″) versus the applied frequency (*f*) for NBR loaded with: a) expanded graphite (EG), b) graphite (G); 1 — 0 phr, 2 — 2 phr, 3 — 4 phr, 4 — 6 phr, 5 — 8 phr, 6 — 10 phr

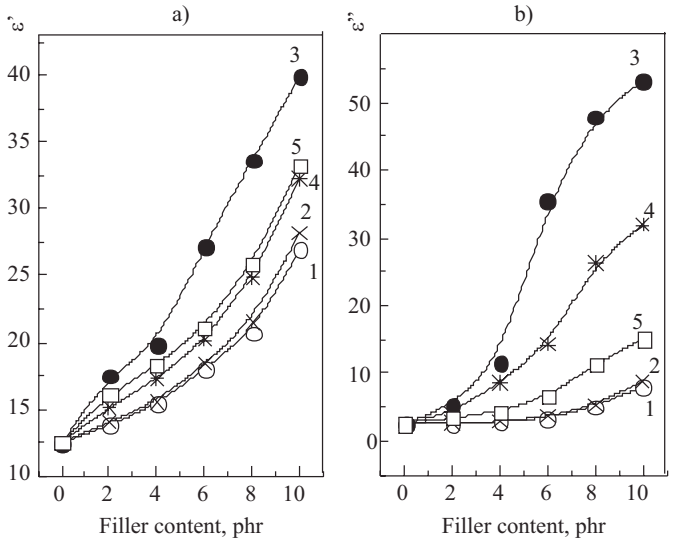

Fig. 8. The permittivity ε′ and dielectric loss ε″ at fixed frequency *f* = 100 Hz for different filler content: 1 — G, 2 — EG, 3 — 30 % PEG, 4 — 50 % PEG, 5 — 70 % PEG

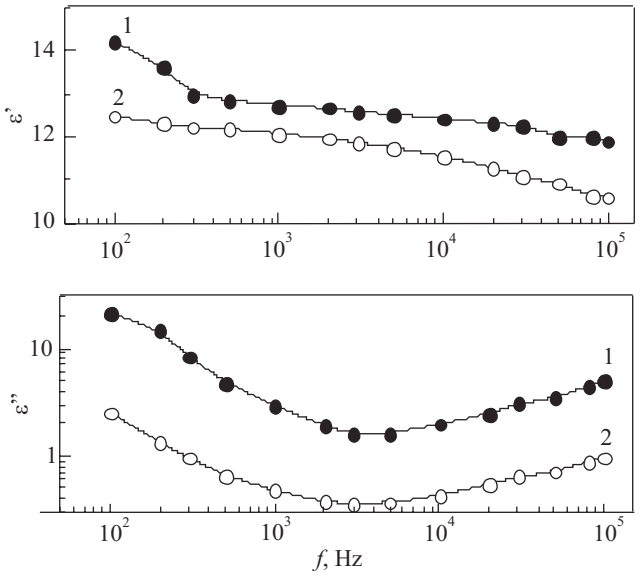

Fig. 9. The permittivity (ε′) and dielectric loss (ε″) versus the applied frequency (*f*) for: 1 — PEG, 2 — NBR

the concentration of EG reaches 8 phr. At this concentration, the tendency of conductivity chain formation increases through the aggregation of the particle networks, whereas at lower concentrations, the particles of filler are widely dispersed throughout the polymer matrix.

Figure 8 represents the variation of permittivity ε′ and dielectric loss ε″ versus filler content at a fixed frequency *f* = 100 Hz. From this figure it is clear that both values increase with higher filler contents but at a certain concentration an abrupt increase in both values occurs. This increase may be due to aggregate formation of G particles inside the NBR matrix. It is seen that the concentration at which the formation of such aggregation, and consequently an abrupt increase, occurs at about 8 phr for both G and EG.

For high performance results, G was treated with PEG aiming to obtain a better distribution of G inside the NBR matrix.

It is well known that the distribution of filler in a polymeric matrix is one of the most important factors affecting the physical properties of the final products [28]. For this reason, the objective of this study was to use polyethylene glycol (PEG) as a dispersing agent to obtain a better distribution of G inside the NBR matrix. It was interesting to measure the dielectric properties of PEG and compare them with those obtained for NBR. Figure 9 depicts the dielectric data for both NBR and PEG, respectively. From this figure it is seen that both permittivity ε′ and dielectric loss ε″ are higher for PEG when compared with NBR. Also, the curves relating ε″ and the applied frequency are broad, indicating the role of more than one relaxation process. The electrical conductivity for both NBR and PEG was calculated from the measured resistivity and found to be $1.32 \cdot 10^{-10}$ and $8.75 \cdot 10^{-10}$ Ω^{-1} cm^{-1}, respectively. This result indicates that PEG possesses lower dc conductivity when compared with that of NBR as it possesses a higher dielectric loss as seen in Fig. 9.

G was treated with PEG at three different ratios (30, 50 and 70 %) and both permittivity ε′ and dielectric loss ε″ were measured in a frequency range 100 Hz to 100 kHz and at 30 °C. The obtained data are illustrated in Fig. 10. From this figure it is seen that both values increase for higher G contents and at a certain content called the percolation threshold, about 6 phr, an abrupt increase was noticed for both values.

To understand such phenomena, both ε′ and ε″ are illustrated graphically versus G content at a fixed frequency *f* = 100 Hz in (Fig. 8). From this figure it is seen that both values decrease with higher PEG contents. This finding recommends 30 wt % of PEG as a dispersing agent for EG. Above this concentration there is a decrease in ε″ values.

Figure 11 represents the electrical conductivity σ of the composites under investigation. From this figure it is clear that σ increases with higher filler contents and an abrupt increase was noticed after 6 phr of filler, which supports the results obtained for both ε′ and ε″. Also, it is interesting to find that the values of the electrical conductivity σ are in the order 10^{-10} Ω^{-1} cm^{-1}, which suggests the use of such composites as antistatic materials [29].

CONCLUSIONS

In this study, nanographite has been synthesized and treated by using poly(ethylene glycol) (PEG) with different concentrations. The TEM photomicrographs provide a clear indication of the formation of nanographite.

The X-ray results suggest that the inter-gallery spacing of pristine graphite increases with the incorporation of the PEG.

The incorporation of EG, treated nanographite and unmodified graphite in NBR matrix shows an improve-

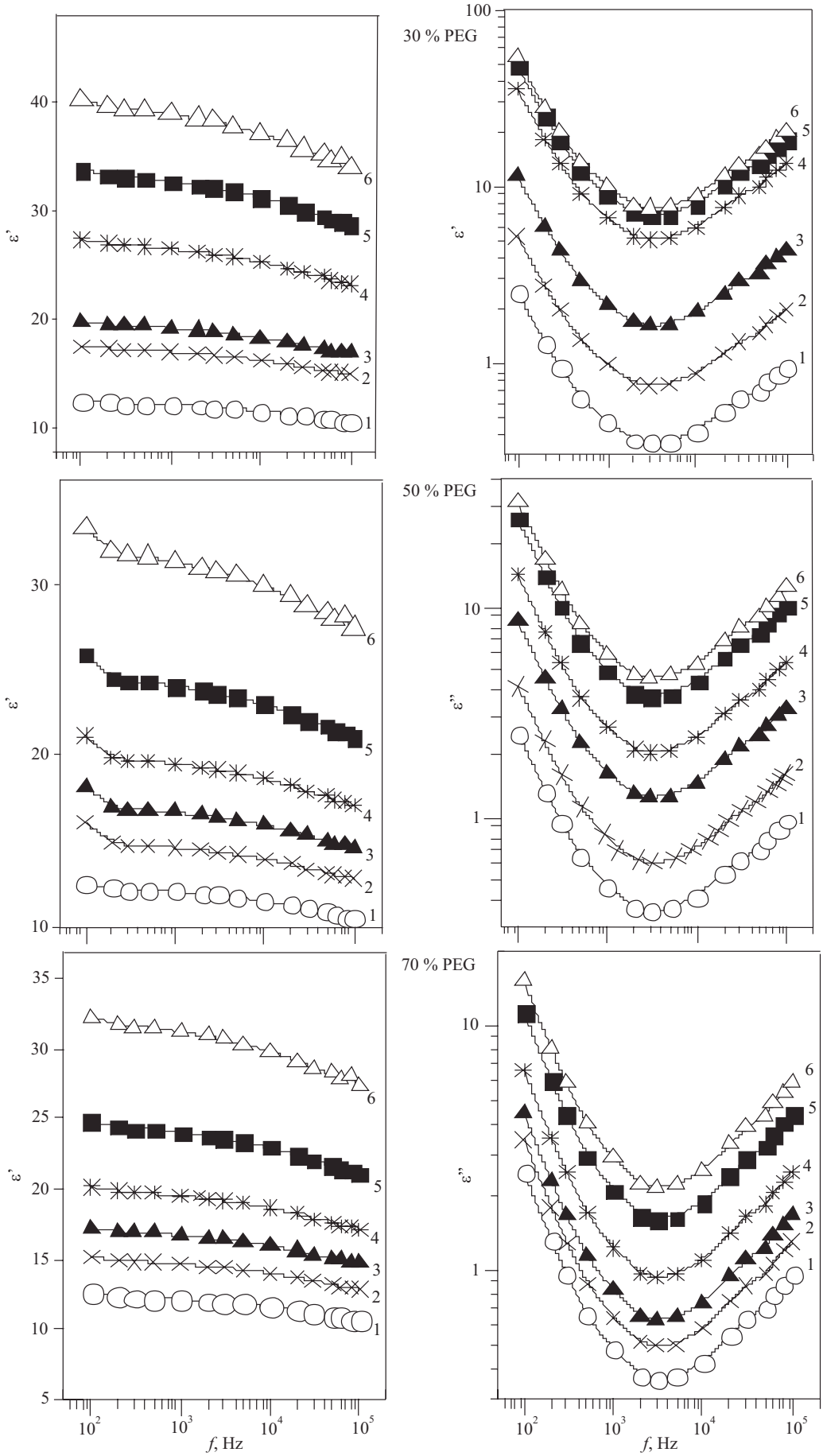

Fig. 10. The permittivity (ε′) and dielectric loss (ε″) versus G content and versus the applied frequency (*f*) for NBR filled with graphite modified with PEG:); 1 — 0 phr, 2 — 2 phr, 3 — 4 phr, 4 — 6 phr, 5 — 8 phr, 6 — 10 phr

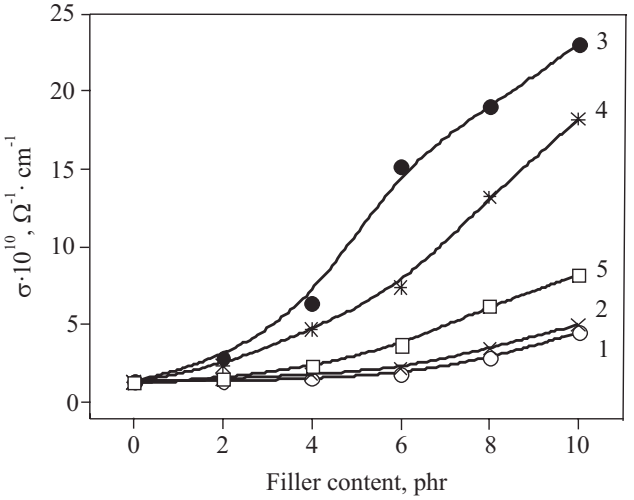

Fig. 11. The electrical conductivity σ versus filler content for NBR: 1 — G, 2 — EG, 3 — 30 wt % PEG, 4 — 50 wt % PEG, 5 — 70 wt % PEG

ment in the rheometric characteristics compared to NBR with unmodified graphite.

Upon the incorporation of EG and treated nanographite, the tensile strength, elongation at break, Young's modulus and hardness of NBR improved, even with a very low degree of filler loading, because of the exfoliation of the clay, as observed in XRD studies.

The thermal stability of the treated nanographite loaded NBR composites studied using thermogravimetric analysis showed an increase in the thermal stability due to the presence of treated nanographite and a higher residual weight percentage than the unmodified graphite.

The dielectric investigations reflect increase in both the permittivity and dielectric loss by increasing filler content.

REFERENCES

[1] Kalaitzidou K., Fukushima H., Lawrence T.D.: *Compos. Sci. Technol.* **2007**, *67*, 2045. http://dx.doi.org/10.1016/j.compscitech.2006.11.014

[2] Wanga L., Zhanga L., Tiana M.: *Wear* **2012**, *276—277*, 85. http://dx.doi.org/10.1016/j.wear.2011.12.009

[3] Song S.H., Jeong H.K., Kang Y.G.: *Ind. Eng. Chem.* **2010**, *16*, 1059. http://dx.doi.org/10.1016/j.jiec.2010.07.004

[4] Zheming Gu., Chunzhong Li., Gengchao W., Ling Z., Qilin C. *et al.*: *J. Ind. Eng. Chem.* **2010**, *16*, 10. http://dx.doi.org/10.1016/j.jiec.2010.01.028

[5] Chen G.H., Wu D., Weng W., Wu C.: *Carbon* **2003**, *41*, 619. http://dx.doi.org/10.1016/S0008-6223(02)00409-8

[6] Chen G.H., Weng W., Wu D., Wu C.: *Euro Polym. J.* **2003**, *39*, 2329. http://dx.doi.org/10.1016/j.eurpolymj.2003.08.005

[7] Chen G.H., Wu C., Weng W., Wu D., Yan W.: *Polym. Commun.* **2003**, *44*, 1781. http://dx.doi.org/10.1016/S0032-3861(03)00050-8

[8] Kenisarin M., Mahkamov K.: *Renew. Sustain. Energy Rev.* **2007**, *11*, 1913. http://dx.doi.org/10.1016/j.rser.2006.05.005

[9] Tyagi V.V., Buddhi D.: *Renew. Sustain. Energy Rev.* **2007**, *11*, 1146. http://dx.doi.org/10.1016/j.rser.2005.10.002

[10] Pasupathy A., Velraj R., Seeniraj R.V.: *Renew. Sustain. Energy Rev.* **2008**, *12*, 39. http://dx.doi.org/10.1016/j.rser.2006.05.010

[11] Wanga W., Yang X., Fang Y., Ding J., Yan J.: *Appl. Energy* **2009**, *86*, 1479. http://dx.doi.org/10.1016/j.apenergy.2008.12.004

[12] Pal K., Rajasekar R., Kang D.J., Zhang Z.X., Pal S.K., Das C.K., Kim J.K.: *Mater. Des.* **2010**, *31*, 677. http://dx.doi.org/10.1016/j.matdes.2009.08.014

[13] Yang J., Tian M., Qing-Xiu J., Li-Qun Z., Xiao-Lin Li.: *J. Appl. Polym. Sci.* **2006**, *102*, 4007. http://dx.doi.org/10.1002/app.24844

[14] Szczepanik M., Stabik J., Łazarczyk M., Dybowska A.: *Arch. Mater. Sci. Eng.* **2009**, *37*, 37.

[15] Certeisen S.R.: *Eng. Plast.* **1996**, *9*, 26.

[16] Weber M., Kamal M.: *Polym. Comp.* **1997**, *6*, 711. http://dx.doi.org/10.1002/pc.10324

[17] Dani A., Ogale A.A.: *Compos. Sci. Technol.* **1996**, *56*, 911. http://dx.doi.org/10.1016/0266-3538(96)00054-1

[18] Abd-El-Messieh S.L., Abd-El-Nour K.N.: *J. Appl. Polym. Sci.* **2003**, *88*, 1613. http://dx.doi.org/10.1002/app.11686

[19] Zhang Z., Zhang N., Peng J., Fang X., Gao X., Fang Y.: *Appl. Energy* **2012**, *91*, 426. http://dx.doi.org/10.1016/j.apenergy.2011.10.014

[20] Mack J.J., Viculis L.M., Ali A., Luoh R., Yang G., Hahn H.T., Ko F.K., Kaner R.B.: *Adv. Mater.* **2005**, *17*, 77. http://dx.doi.org/10.1002/adma.200400133

[21] Wang Y.T., Wang C.S., Yin H.Y., Wang L.L., Xie H.F., Cheng R.S.: *eXPRESS Polym. Lett.* **2012**, *6* (*9*), 719. http://dx.doi.org/10.3144/expresspolymlett.2012.77

[22] Song S.H., Jeong H.K., Kang Y.G.J.: *Ind. Eng. Chem.* **2010**, *16*, 1059. http://dx.doi.org/10.1016/j.jiec.2010.07.004

[23] Yang J., Tian M., Jia Q.X., Shi J.H., Zhang L.Q., Lim S.H., Yu Z.Z., Mai Y.W.: *Acta Mater.* **2007**, *55*, 6372. http://dx.doi.org/10.1016/j.actamat.2007.07.043

[24] Wang L., Zhang L.Q., Tian M.: *Mater. Des.* **2012**, *39*, 450. http://dx.doi.org/10.1016/j.matdes.2012.02.051

[25] Amraee I.A., Katbab A.A., Aghafarajollah S.H.: *Rubber Chem. Technol.* **1995**, *69*, 130. http://dx.doi.org/10.5254/1.3538353

[26] Leyva M.E., Barra G.M.O., Moreira A.C.F., Soares B.G., Khastgir D.: *J. Polym. Sci., Part B* **2003**, *41*, 2983. http://dx.doi.org/10.1002/polb.10627

[27] Reffaee A.S.A., El-Nashar D.E., Abd-El-Messieh S.L., Abd-El Nour K.N.: *Mater. Des.* **2009**, *30*, 3760. http://dx.doi.org/10.1016/j.matdes.2009.02.001

[28] Sirisinha C., Prayoonchatphan N.: *J. Appl. Polym. Sci.* **2001**, *81*, 3198. http://dx.doi.org/10.1002/app.1773

[29] Margolis J.M.: "In Conductive Polymers and Plastics", Chapman and Hall, New York 1989.

Received 22 X 2013.